Journal of ASTM International, Vol. 8, No. 2
Paper ID JAI103378
Available online at www.astm.org

Wenhua Yu,[1] *David M. France,*[2] *and Jules L. Routbort*[3]

Forced Convective Boiling of Ethylene Glycol/Water Mixtures Inside a Small Tube

ABSTRACT: Forced convective boiling heat transfer of water and ethylene glycol/water mixtures with volume concentration ratios of 40/60, 50/50, and 60/40 in a 2.98-mm inner-diameter circular tube has been investigated for both horizontal and vertical upward flows. Boiling heat transfer rates of the test fluids were determined experimentally over a range of mass flux, vapor mass quality, and inlet subcooling through a boiling data reduction procedure that allowed analytical calculation of the fluid boiling temperatures along the experimental test section by applying ideal mixture and equilibrium assumptions along with Raoult's law. Based on the experimental findings that the heat flux in the nucleation-dominant-boiling region was dependent strongly on the wall superheat but almost independent of the mass flux and the inlet subcooling, prediction equations were developed for boiling heat transfer coefficients of water and ethylene glycol/water mixtures in small channels. The equations predict the experimental data well, and most of the predicted values are within ±30 % of the experimental data.

KEYWORDS: forced convective boiling, heat transfer, ethylene glycol/water mixture

Nomenclature

Indices

bubble = bubble point
dew = dew point
EG = ethylene glycol
f = fluid
in = inlet
l = liquid
out = outlet
sat = saturation
v = vapor
W = water
w = wall

Latin Symbols

Bo = boiling number
C_p = specific heat
d_i = inside diameter
d_o = outside diameter
E = voltage drop
F = mass concentration
f = friction factor
G = mass flux
h = heat transfer coefficient
I = current

Manuscript received September 14, 2010; accepted for publication January 5, 2011; published online February 2011.
[1] Energy Systems Division, Argonne National Laboratory, 9700 South Cass Ave., Argonne, IL 60439, e-mail: wyu@anl.gov
[2] Dept. of Mechanical and Industrial Engineering, Univ. of Illinois at Chicago, 842 West Taylor St., Chicago, IL 60607, e-mail: dfrance@uic.edu
[3] Energy Systems Division, Argonne National Laboratory, 9700 South Cass Ave., Argonne, IL 60439, e-mail: routbort@anl.gov

Copyright © 2011 by ASTM International, 100 Barr Harbor Drive, PO Box C700, West Conshohocken, PA 19428-2959.

i	enthalpy
i_{fg}	latent heat of vaporization
k	thermal conductivity
L	length
M	molecular mass
$\dot{m}$	mass flowrate
Nu	Nusselt number
p	pressure
Pr	Prandtl number
Q	volumetric flowrate
$\dot{q}$	heat transfer rate
$\dot{q}''$	heat flux
Re	Reynolds number
T	temperature
T'_w	outer surface wall temperature
V	volume concentration
We	Weber number
x	vapor mass quality
Y	molar concentration
z	axial location

Greek Symbols

Δp	pressure drop
Δq	heat input to a segment
ΔT_{sat}	wall superheat
$\rho =$	density
$\sigma =$	surface tension

Introduction

Currently, cooling systems in heavy vehicles are designed to use a 50/50 ethylene glycol/water (EG/W) mixture in the liquid state. Most of the heat is transferred in the radiator to the heat sink ambient air. The amount of the heat rejected in the radiator is limited by current radiator designs that are essentially optimal. In addition, precision cooling using the 50/50 EG/W liquid mixture is limited by the coolant liquid properties and the cooling system geometry. Because of its order-of-magnitude higher heat transfer rates, there is interest in using controllable two-phase nucleate boiling instead of conventional single-phase forced convection in vehicular cooling systems under certain conditions or in certain areas of the engine to remove ever increasing heat loads and to eliminate potential hot spots in engines [1–15].

Order-of-magnitude higher heat transfer rates can be achieved in nucleate-boiling cooling systems when compared with conventional, single-phase, and forced convective cooling systems. However, successful designs and applications of nucleate-boiling cooling systems for engine applications require that two conditions be met: The critical heat flux not to exceed and flow instability not to occur. Therefore, a fundamental understanding of flow boiling mechanisms under engine application conditions is required to develop reliable and effective nucleate-boiling cooling systems. Cooling engine areas such as the head region often contain small metal masses that lead to small coolant channels. This geometry, in turn, leads to low mass flow rates that minimize pressure drops. Although significant research has been performed on the boiling heat transfer and the critical heat flux phenomena, the fundamental understanding of the two-phase flow and the heat transfer of a 50/50 EG/W mixture under engineering application conditions is still limited. In addition, it is not practical to precisely maintain the volume concentration ratio of the EG/W mixture coolant at 50/50. Therefore, any investigation into engine coolant characteristics should

include a range of volume concentration ratios around the nominal 50/50 mark. The objectives of this study are to experimentally investigate the characteristics of two-phase forced convective boiling heat transfer under conditions of small channels and low mass fluxes for distilled water and EG/W mixtures with volume concentration ratios of 40/60, 50/50, and 60/40 in both horizontal and vertical upward flows and to develop predictive methods for the two-phase forced convective boiling heat transfer coefficient under these engine application conditions.

Experimental Apparatus

Description of Two-Phase Experimental Apparatus

The experimental apparatus used in this study is a closed-loop system consisting of two pumps, a hydraulic accumulator, a flowmeter set, a preheater, two similar experimental test sections (one for horizontal flow and one for vertical flow), and a condenser. As shown in the schematic diagram of the experimental apparatus in Fig. 1, the test fluid was pumped through the two-phase loop by two serially arranged pumps (Micropump Corporation, Model 220-000) and was pressurized by a bladder-type hydraulic accumulator (Greer Hydraulics, Inc.) connected to a high-pressure nitrogen cylinder. The serially arranged pumps driven by alternating current adjustable-frequency drives (Dayton Electric Manufacturing Co., Model 1XC95) allowed fine flow adjustments that minimized flow fluctuations caused by the boiling fluid in the experimental test section. The bladder-type accumulator provided stable pressure control in the test apparatus. The flowmeter set, including a piston-type flowmeter with a readout-meter (Max Machinery, Inc., Model 213-310/Model 120-200), a turbine-type flowmeter with a readout-meter (Flowdata, Inc., Model ES02SS-6FM-DL-102-00/Model MR10-1A3A), and a rotameter (Omega Engineering, Inc., Model FL-3505ST-HRV), was arranged in a parallel-flow configuration in the experimental apparatus and was chosen to cover a large range of volumetric flowrates (Q). A thermocouple probe (T_{FM}) (Omega Engineering, Inc.) just upstream from the flowmeter set provided a means to determine the density of the fluid and subsequently the mass flowrate of the fluid. Exiting the flowmeter set, the fluid flowed through the preheater in which the fluid temperature was raised to the desired subcooled level for a given test. The preheater, consisting of an American Iron and Steel Institute (AISI) type 304 stainless steel tube with a 4.572-mm inside diameter, a 6.096-mm outside diameter, and a 500-mm resistance-heated length, was heated by passing current through its wall to generate resistance heat with a direct current power supply (Sorensen Co., Model DCR 16-625T). As a safety precaution for protecting the preheater from overheating, the preheater was provided with a temperature interlock. The wall temperature (T_5) was measured and then fed to a high-temperature limit switch (Omega Engineering, Inc., Model CN76030) that would terminate power to the preheater when a preset upper-temperature limit was reached. After passing through the preheater, the fluid entered either the horizontal or the vertical experimental test section. The experimental test section was heated by passing current through its wall with a direct current power supply (Electronic Measurements, Inc., Model EMHP 40-450-D-11111-0933). The voltage drop across the experimental test section (E) was measured directly, and the current through the experimental test section (I) was determined from a measurement of the voltage drop across a shunt resistor with known resistance of 0.0001 Ω. The heat input to the experimental test section was determined from these two measurements. Electrical isolation for eliminating ground loops was provided for the preheater and the experimental test section by short high-pressure hoses, designated isolation in Fig. 1. Immediately beyond the experimental test section, a flow sight glass window provided a view of the flow pattern. The two-phase fluid flowing out from the experimental test section was condensed into a single-phase fluid in the countercurrent condenser that used laboratory water as a heat rejection fluid. The condensate left the condenser and returned to the pumps to close the loop.

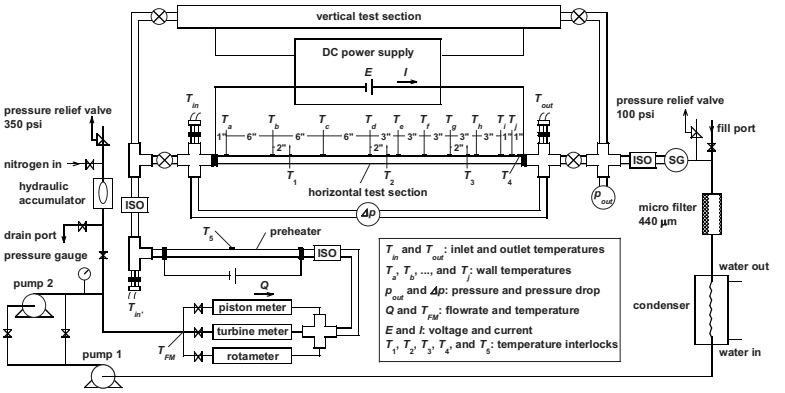

FIG. 1—*Schematic diagram of experimental apparatus.*

Experimental Test Section

The details of the horizontal experimental test section (the setup for the vertical experimental test section is the same) are shown schematically in Fig. 1. The experimental test section was fabricated from a 2.9845-mm-inside-diameter (d_i) and 4.7625-mm-outside-diameter (d_o) AISI type 316 stainless steel tube with a 0.9144-m heated length (L) between the voltage taps. The in-stream bulk fluid temperatures were measured at the inlet (T_{in}) and the outlet (T_{out}) of the experimental test section with type K thermocouple probes (Omega Engineering, Inc. KMTSS-062U-6). A small outside diameter of 1.5748 mm was selected to minimize flow effects.

Figure 1 also illustrates the method used to measure wall temperatures ($T_a, T_b, \ldots, T_j$) at 10 axial locations over the heated length of the experimental test section with type K thermocouple junctions (Omega Engineering, Inc.). To electrically isolate these thermocouple junctions from the experimental test section tube, a thin coat of high-temperature ceramic epoxy (Omega Engineering, Inc., Omega bond 200) was applied around the circumference of the tube at the measurement locations. After oven curing, the thermocouple junctions coated with the same high-temperature ceramic epoxy were bonded to the thin coating on the tube. This technique allowed the thermocouple junctions to be electrically insulated from the tube that had current passing through it, and it provided low thermal resistance between the junctions and the tube.

The outlet fluid pressure (p_{out}) and the overall pressure drop across the test section (Δp) were measured in all tests with a piezoelectric pressure transducer (Endevco Corporation, Model 8510B-500) and a differential pressure transducer with variable reluctance (Validyne Engineering Corporation, Model DP15-36 1536N1S4A), respectively. These measurements were incorporated in the data reduction to calculate the stream temperature distribution along the boiling segment of the experimental test section. As a safety precaution for protecting the experimental test section from overheating, the experimental test section was provided with temperature interlocks similar to the preheater interlock.

Instrumentation Calibration

All the sensors for the measurements of flowmeter temperature, in-stream bulk fluid temperature, wall temperature, fluid pressure at the outlet of the experimental test section, overall pressure drop across the experimental test section, and volumetric flowrate were calibrated before installation.

The flowmeter thermocouple probe, the in-stream temperature probes, and the wall thermocouple junctions were calibrated over the operation range with a type K reference probe (Omega Engineering Inc., No. 703998035), which was calibrated with a National Institute of Standards and Technology (NIST)-traceable standard. In addition, a system calibration, including the multiplexor and the computer was performed. The estimated uncertainty in the measurement of temperatures was $\pm 0.2\,^{\circ}\text{C}$.

The pressure transducers were calibrated over the operation range using a precise pressure gauge (Ashcroft, Inc., Model Hiese CM-21615), which was calibrated with a NIST-traceable standard. As with the thermocouples, the pressure transducers were calibrated through the multiplexor and the computer. The estimated uncertainty in the measurement of pressures was ± 3 %.

The flowmeters were calibrated over the operation range using a weighing-with-stop-watch technique

at the temperatures at which the flowrate measurements for single-phase and boiling heat transfer experiments were made. The estimated uncertainty in the measurements of flowrates was ±3 %. Correction equations were developed for all sensors based on the calibration data and were incorporated into the data acquisition program.

Data Acquisition

A data acquisition system consisting of a personal computer and a multiplexor (Hewlett-Packard Co., Model 3421A) was assembled to record outputs from all sensors. A data acquisition program, including all calibration equations and engineering-unit conversions, was written. The data acquisition system functioned in two modes. During experimental test setup, the data acquisition system provided an on-screen display of analog signals from all sensors and graphs of representative temperature and flowrate measurements as a function of time to facilitate determination of steady-state conditions. When the system reached a steady-state condition at desired parameters, the data acquisition system read all sensor-output voltages of in-stream temperatures, wall temperatures, outlet pressure, pressure drop, volumetric flowrate, voltage drop, and current 30 times and averaged them in three sets of 10-data scans each. As a check on the steady-state condition, the three data sets were compared for consistency before all of the scans were averaged together for future processing. The final result was a set of measurements, each an average of 30 readings, plus a confirmation of steady-state system operation during the collection of data.

Heat Loss Calibration

Although the experimental test section was well insulated thermally from the atmosphere to minimize heat loss to the environment, the heat loss was not negligible during flow boiling heat transfer tests because of the small experimental test section, the low fluid flowrates, and the relatively high driving temperatures. Therefore, heat loss tests were performed for the experimental test section wall temperatures up to the boiling heat transfer conditions, and the heat loss was subsequently incorporated into the data reduction procedure for boiling heat transfer data. It was found that the test section heat loss was <5 % of the applied input power to the experimental test section in all subsequent heat transfer tests.

Single-Phase Heat Transfer Verification

To validate the test apparatus, a series of single-phase heat transfer experiments was carried out before two-phase flow boiling experiments. The single-phase heat transfer experiments were performed at a system pressure of 120–200 kPa, sufficient to keep the test fluids in the liquid phase during heating. During the single-phase heat transfer experiments, the experimental parameters of the test fluids such as temperatures and flowrates were chosen to maintain turbulent flow conditions with their Reynolds numbers >2000. The results of the single-phase Nusselt numbers Nu for the Reynolds numbers in the range of $\mathrm{Re}=3000-13\,000$ and the Prandtl numbers in the range of $\mathrm{Pr}=2-18$ were compared with the well-known Gnielinski equation [16]

$$\mathrm{Nu} = \frac{(f/8)(\mathrm{Re}-1000)\mathrm{Pr}}{1+12.7(f/8)^{1/2}(\mathrm{Pr}^{2/3}-1)} \tag{1}$$

where the friction factor f is

$$f = (1.82 \log \mathrm{Re} - 1.64)^{-2} \tag{2}$$

As shown in Fig. 2, where the local Nusselt numbers are plotted, the experimental data are in good agreement with the predicted values from the Gnielinski equation with a mean deviation of <7 %. Almost all experimental data are within ±15 % of the predictions. These single-phase heat transfer coefficient results serve as validation of the accuracy of the instrumentation, measurements, data acquisition, and data reduction procedures. They are an “end-to-end” final validation of the experimental apparatus.

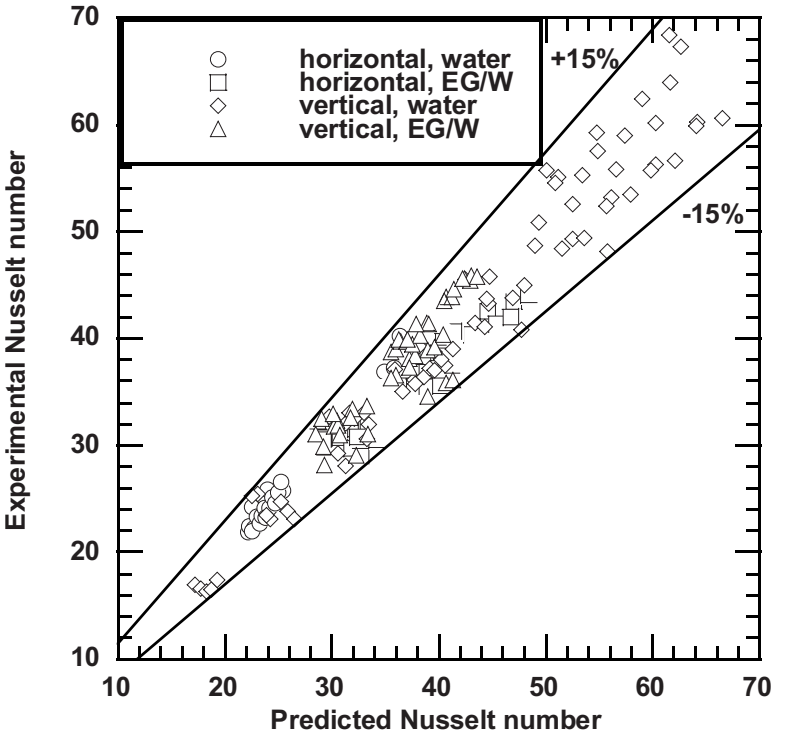

FIG. 2—*Single-phase heat transfer compared to Gnielinski equation predictions.*

Boiling Data Reduction

Ideal Mixture Assumption

EG/W mixtures are nonazeotropic mixtures. The solid lines of Fig. 3 are an example of their composition-temperature phase diagram at a constant pressure $p=100$ kPa [17]. The bubble point line and the dew point line divide the phase diagram into three regions: Subcooled liquid, two-phase fluid, and superheated vapor. For a given EG/W mixture with water molar concentration Y_W, the boiling starts at the bubble point temperature T_{bubble} with the water liquid molar concentration and the water vapor molar concentration $Y_{Wl\text{bubble}}$ ($Y_{Wl\text{bubble}}=Y_W$) and $Y_{Wv\text{bubble}}$, respectively. The mixture liquid phase becomes richer in the less-volatile-component, ethylene glycol, while its vapor phase becomes richer in the more-volatile-component, water. As the boiling process continues, the mixture vapor mass quality gradually increases from 0 to 1, the mixture temperature increases from the bubble point T_{bubble} to the dew point T_{dew}, and the water liquid molar concentration and the water vapor molar concentration of the mixture change into $Y_{Wl\text{dew}}$ and $Y_{Wv\text{dew}}$ ($Y_{Wv\text{dew}}=Y_W$), respectively. As evident from the phase diagram, unlike pure fluids, the mixture boiling process at a constant pressure does not occur at a constant temperature but rather over a range of temperatures from the bubble point T_{bubble} through the dew point T_{dew}, depending on the mixture vapor mass quality. This significant feature means that further information, in addition to the system pressure, is needed to calculate the boiling temperature and subsequently the heat transfer coefficient.

In this study, forced convective boiling experiments were performed in a small diameter circular tube, and boiling heat transfer data were obtained in the mixture vapor mass quality range away from the occurrence of the critical heat flux. Consequently, the two-phase regions of bubble, slug, and annular flows were present along the experimental test section in various experiments in which the liquid was adjacent to the heated experimental test section wall at all times. These two-phase flow regions are relatively well mixed with small thermal gradients compared to the post-critical heat flux mist flow region where vapor is adjacent to the wall. Therefore, for the purpose of data reduction in this study, the assumption was made that, in the thermodynamic sense, the mixture behaves ideally and is at equilibrium. In support of this assumption, Raoult's law for ideal mixtures was used to generate a phase diagram for EG/W mixtures at a constant pressure $p=100$ kPa. The results, plotted as dashed lines in Fig. 3, show that the calculated values are very close to the data (solid lines) [17] with a mean deviation of <4.7 %.

To calculate local boiling heat transfer coefficients of an EG/W mixture, the ethylene glycol vapor

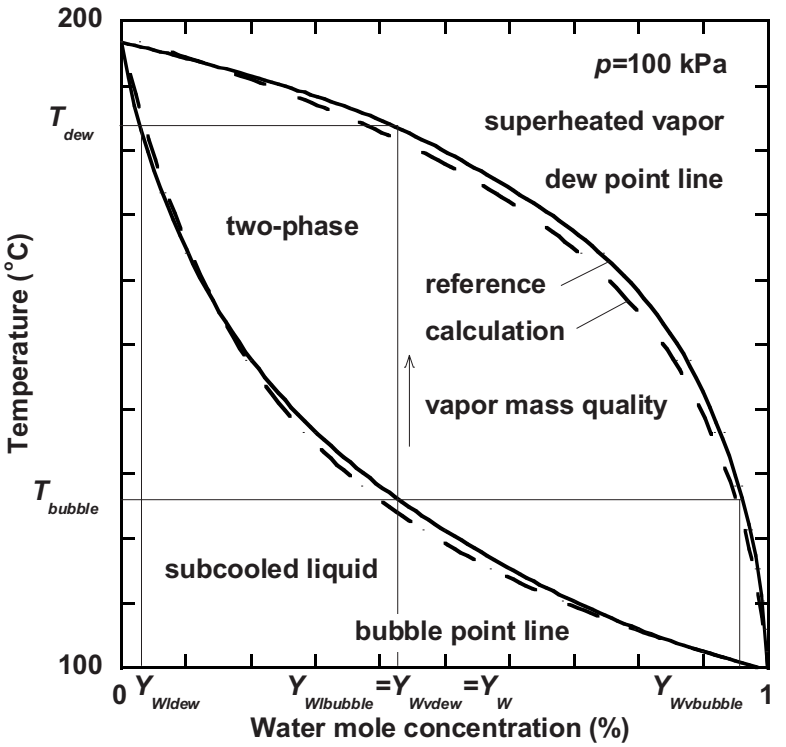

FIG. 3—*EG/W mixture phase diagram.*

mass concentration, the mixture vapor mass qualities, and the mixture temperatures along the experimental test section must be determined. Perhaps the simplest approach is to assume that the fluid boiling temperature is constant along the experimental test section and equals the mean of the temperature at the zero vapor mass quality location and the temperature at the experimental test section outlet. Such an approach was taken by Murata and Hashizume [18] in the analysis of nonazeotropic refrigerant mixtures. However, this approach is not conducive to the determination of the local boiling heat transfer coefficients along the length of the experimental test section, as in this study. Accuracy can be increased by assuming a linear fluid temperature distribution along the experimental test section as done by Wenzel et al. [19] for ternary mixtures. Still another approach is to utilize a fluid equation of state such as the hard sphere equation developed by Morrison and McLinden [20] and used by Ross et al. [21] for refrigerant mixtures. However, analyses show that the ideal mixture assumption and the equilibrium assumption are sufficient to calculate the fluid boiling temperatures along the experimental test section and subsequently the local boiling heat transfer coefficients. Therefore, this approach was adopted in the present study.

Boiling Heat Transfer Coefficient Calculation

By considering the two-phase EG/W mixture over a segment of the experimental test section shown in Fig. 4, the ideal mixture assumption and the equilibrium assumption along with Raoult's law give [22]

$$Y_{\mathrm{EG}v} = \frac{p_{\mathrm{EGsat}}}{p} Y_{\mathrm{EG}l} = \frac{p_{\mathrm{EGsat}}}{p} \frac{p - p_{\mathrm{Wsat}}}{p_{\mathrm{EGsat}} - p_{\mathrm{Wsat}}} \tag{3}$$

where:

p = pressure,
Y = molar concentration,
EG = ethylene glycol,
l = liquid,
sat = saturation,
v = vapor, and
W = water.

The species conservation of the ethylene glycol in the mixture gives

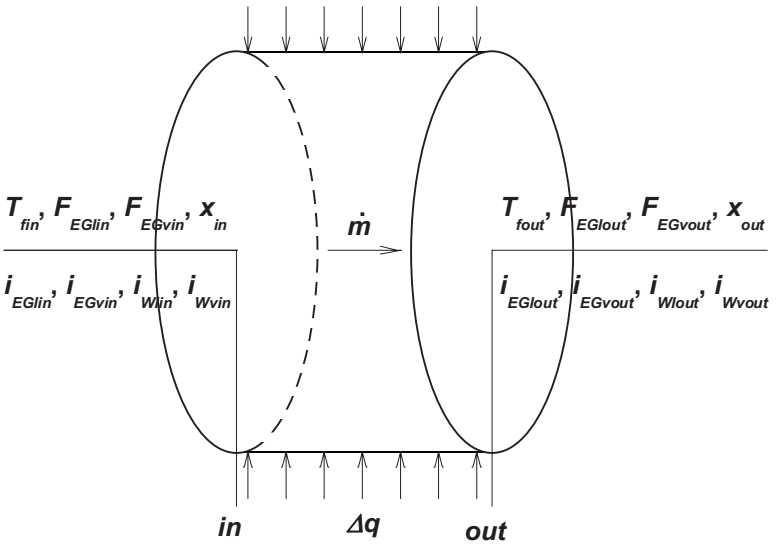

FIG. 4—*A segment of the experimental test section.*

$$F_{\mathrm{EG}} = (1 - x)F_{\mathrm{EG}l} + xF_{\mathrm{EG}v} \tag{4}$$

where:

F = mass concentration, and
x = vapor mass quality.

The energy conservation of the EG/W mixture over the segment length gives

$$\begin{aligned}\Delta q = \dot{m}\{&[(1 - F_{\mathrm{EG}l\mathrm{out}})(1 - x_{\mathrm{out}})i_{\mathrm{W}l\mathrm{out}} + F_{\mathrm{EG}l\mathrm{out}}(1 - x_{\mathrm{out}})i_{\mathrm{EG}l\mathrm{out}} + (1 - F_{\mathrm{EG}v\mathrm{out}})x_{\mathrm{out}}i_{Wv\mathrm{out}} + F_{\mathrm{EG}v\mathrm{out}}x_{\mathrm{out}}i_{\mathrm{EG}v\mathrm{out}}] \\ &- [(1 - F_{\mathrm{EG}l\mathrm{in}})(1 - x_{\mathrm{in}})i_{\mathrm{W}l\mathrm{in}} + F_{\mathrm{EG}l\mathrm{in}}(1 - x_{\mathrm{in}})i_{\mathrm{EG}l\mathrm{in}} + (1 - F_{\mathrm{EG}v\mathrm{in}})x_{\mathrm{in}}i_{Wv\mathrm{in}} + F_{\mathrm{EG}v\mathrm{in}}x_{\mathrm{in}}i_{\mathrm{EG}v\mathrm{in}}]\}\end{aligned} \tag{5}$$

where:

i = enthalpy,
$\dot{m}$ = mass flowrate,
Δq = heat input to the segment,
in = inlet to the segment, and
out = outlet to the segment.

By solving the above equations, the ethylene glycol vapor mass concentration $F_{\mathrm{EG}v}$ can be obtained

$$F_{\mathrm{EG}v} = \frac{31(p_{\mathrm{EGsat}}/p)F_{\mathrm{EG}l}}{31 - 22(1 - p_{\mathrm{EGsat}}/p)F_{\mathrm{EG}l}} = \frac{31(p_{\mathrm{EGsat}}/p)(p - p_{\mathrm{Wsat}})}{9(p_{\mathrm{EGsat}} - p_{\mathrm{Wsat}}) + 22(p_{\mathrm{EGsat}}/p)(p - p_{\mathrm{Wsat}})} \tag{6}$$

where the following conversion to molecular mass M was used:

$$F_{\mathrm{EG}} = \frac{Y_{\mathrm{EG}}}{M_W/M_{\mathrm{EG}} + (1 - M_W/M_{\mathrm{EG}})Y_{\mathrm{EG}}} \tag{7}$$

The vapor mass quality x can also be obtained

$$x = \frac{F_{\mathrm{EG}l} - F_{\mathrm{EG}}}{F_{\mathrm{EG}l} - F_{\mathrm{EG}v}} = 1 - \frac{F_{\mathrm{EG}} - F_{\mathrm{EG}v}}{F_{\mathrm{EG}l} - F_{\mathrm{EG}v}} = 1 - \frac{[31 + 22(p/p_{\mathrm{EGsat}} - 1)F_{\mathrm{EG}v}](F_{\mathrm{EG}} - F_{\mathrm{EG}v})}{(p/p_{\mathrm{EGsat}} - 1)(31 - 22F_{\mathrm{EG}v})F_{\mathrm{EG}v}} \tag{8}$$

The EG/W mixture temperature at the inlet of the segment $T_{f\mathrm{in}}$ can be obtained from the EG/W mixture latent heat of vaporization i_{fg} and the known EG/W mixture temperature at the outlet of the segment $T_{f\mathrm{out}}$

$$T_{f\mathrm{in}} = T_{f\mathrm{out}} - \frac{\Delta q/\dot{m} + [(1 - F_{\mathrm{EG}v\mathrm{in}})i_{fgW\mathrm{in}} + F_{\mathrm{EG}v\mathrm{in}}i_{fgEG\mathrm{in}}]x_{\mathrm{in}} - [(1 - F_{\mathrm{EG}v\mathrm{out}})i_{fgW\mathrm{out}} + F_{\mathrm{EG}v\mathrm{out}}i_{fg\mathrm{EGout}}]x_{\mathrm{out}}}{[(1 - F_{\mathrm{EG}})C_{pWl} + F_{\mathrm{EG}}C_{p\mathrm{EG}l}]} \tag{9}$$

where the enthalpy differences $(i_{Wl\mathrm{out}} - i_{Wl\mathrm{in}})$ and $(i_{\mathrm{EG}l\mathrm{out}} - i_{\mathrm{EG}l\mathrm{in}})$ were approximated over a small incremental length by the products of the specific heat C_p and the temperature difference $C_{pWl}(T_{\mathrm{out}} - T_{\mathrm{in}})$ and $C_{p\mathrm{EG}l}(T_{\mathrm{out}} - T_{\mathrm{in}})$, respectively.

Finally, the local boiling heat transfer coefficient $h(z)$ at position z along the length of the experimental test section is defined as

$$h(z) = \frac{\dot{q}''(z)}{T_w(z) - T_f(z)} \tag{10}$$

where the local heat flux $\dot{q}''(z)$ was calculated from the overall input heating power by using the electrical resistivity of the AISI type 316 stainless steel as a function of the temperature; the local EG/W mixture temperature $T_f(z)$ was calculated at the location of the wall-temperature measurement with the method presented above, and the inner wall surface temperature $T_w(z)$ was determined from a radial heat conduction calculation by using the measured outer surface temperature $T'_w(z)$ and the local heat generation rate $\dot{q}(z)$ in the wall with the known thermal conductivity $k_w(z)$ as a function of the temperature

$$T_w(z) = T'_w(z) + \frac{\dot{q}(z)}{4\pi k_w(z)L}\frac{1 + \ln(d_i/d_o)^2 - (d_i/d_o)^2}{1 - (d_i/d_o)^2} \tag{11}$$

Iteration Calculation Procedure

The data reduction was facilitated by dividing the experimental test section into ten segments corresponding to the locations of the wall thermocouples, and the data reduction proceeded starting from the exit of the experimental test section. With the measured fluid temperature and the measured system pressure at the exit of the experimental test section, the ethylene glycol vapor mass concentration and the vapor mass quality were calculated from Eqs 6 and 8, respectively. By using these values as the outlet parameters of the segment, the inlet values were calculated upstream at the location of the nearest wall thermocouple. Because of the nonlinear relations among the parameters, iteration was used in arriving at the final results. This iteration calculation procedure continued over the incremental segments until the furthest upstream wall thermocouple was reached. In the above calculation, the system pressures at the locations of the wall thermocouples were calculated by assuming a linear pressure distribution with little error because two-phase pressure drops in the experimental test section were small in all experiments (<50 kPa). Finally, the local heat transfer coefficients were found from Eq 10. Based on the uncertainties in each of the independent variables, the uncertainties in heat transfer coefficients were estimated <5 % by using the method of sequential perturbation [23]. In this way, the heat transfer coefficients together with the other parameters were obtained at multiple local conditions along the experimental test section for every test.

Results and Discussions

Ranges of Experimental Parameters

A series of experiments was carried out to investigate two-phase forced convective boiling heat transfer characteristics under conditions of small channels and low mass fluxes for distilled water and EG/W mixtures with volume concentration ratios of 40/60, 50/50, and 60/40 in both horizontal and vertical upward flows. In these experiments, the preheater power supply was adjusted to keep the test fluid inlet temperature at the experimental test section at a desired subcooled point. The experimental test section power supply was increased progressively until the critical heat flux or the preset upper-temperature limit was reached when the system experienced two-phase flow instability. During each test section power supply increase, the measurements of in-stream temperatures, wall temperatures, outlet pressure, pressure drop, volumetric flowrate, voltage drop, and current were recorded for future data reduction. The detailed experimental parameters are: Outlet pressure of $\sim$150 and $\sim$200 kPa, inlet temperature of 20–80°C,

mass flux of 30–200 kg/m^2 s, heat flux of 5–300 kW/m^2, vapor mass quality of 0–1, liquid Reynolds number of <1600, vapor Reynolds number of >2000, and liquid Prandtl number of 1.4–8.3.

Mass Flux Effects and Three Boiling Regions

It has been shown in previous studies for water and EG/W mixture boiling in a small diameter horizontal tube that there exist three flow boiling regions: Convection-dominant boiling, nucleation-dominant boiling, and transition boiling [22,24]. The same phenomenon also exists for water and EG/W boiling in vertical upward flow as seen from Fig. 5 where the effects of the mass flux on the exit boiling curve of water and 50/50 EG/W mixture are shown for five mass flux levels. At low wall superheats, usually less than a few degrees Celsius, the heat fluxes are relatively independent of the wall superheat, and the situation is characterized as the convection-dominant-boiling region. At high wall superheats, the system moves into the transition-boiling region in which the wall temperatures show oscillations, the heat fluxes separate as a function of the mass flux, and the flow boiling is susceptible to flow instabilities. At high enough wall superheats, the critical heat flux condition is reached. For water flow boiling, the highest wall-superheat data obtained in Fig. 5(*a*) were limited by reaching the critical heat flux condition, which is clearly a function of the mass flux. For EG/W mixture flow boiling, which was less stable than for water flow boiling under similar experimental conditions, the highest wall-superheat data obtained in Fig. 5(*b*) were generally limited by excessively large-amplitude flow oscillations and the critical heat flux was almost never attainable. Between these two boiling regions of convection-dominant and transition, there is an extensive nucleation-dominant-boiling region that is the focus of this study.

The nucleation-dominant-boiling region shown in Fig. 5 is typical in small-channel flow boiling and is considerably more extensive than that found in larger-channel flow boiling. In the nucleation-dominant-boiling region, the heat fluxes follow a strong power-law trend of the wall superheat nearly independent of the mass flux, which implies that the nucleate-boiling heat transfer coefficients up to the transition-boiling region are a function of the heat flux only and not a function of the mass flux. This phenomenon, which is the same as findings for refrigerant flow boiling in small channels [25], is attributed to the large slug-flow regime found in small-channel two-phase flows [26], which gives rise to the domination of the nucleation heat transfer mechanism and the minimization of the convective heat transfer mechanism over a large mass flux range. Small-channel flow boiling is usually confined to relatively low mass fluxes due to pressure-drop restrictions, which also contributes to the minimization of the convection contribution to flow boiling heat transfer. These results were incorporated into the correlation of the boiling heat transfer data (presented subsequently) in the nucleation-dominant-boiling region that is the generally desired operating region for flow boiling in small channels due to its relatively high heat transfer rates and flow stability. It should be noted that while the heat fluxes of EG/W mixture flow boiling follow a power-law trend nearly independent of the mass flux similar to water flow boiling, the magnitude of the heat fluxes and therefore the heat transfer rates for EG/W mixture flow boiling fall below that for water flow boiling at the same wall superheats.

Generally, the nucleation-dominant-boiling region may be defined in terms of the wall superheat ΔT_{sat} being between the lower wall-superheat limit $(\Delta T_{sat})_{lower}$ and the upper wall-superheat limit $(\Delta T_{sat})_{upper}$

$$(\Delta T_{sat})_{lower} \leq \Delta T_{sat} \leq (\Delta T_{sat})_{upper} \tag{12}$$

where the lower wall-superheat limit has been found to be approximately a constant and was taken as $2°C$ for all the test fluids and the test conditions in this study. The upper wall-superheat limit is usually a function of the mass flux and should be determined based on the test fluids. This upper wall-superheat limit is shown in Fig. 5 as a solid line dividing the nucleation-dominant-boiling region and the transient-boiling region.

In addition to the key influential factor mass flux, the effects of other experimental parameters of this study on the exit boiling curve were also analyzed and can be summarized as the following: (a) The system pressure has a very slight effect on the exit boiling curves for the two test section outlet pressures of 150 and 200 kPa; (b) under the current test conditions, the exit boiling curves are insensitive to the test section inlet temperature although changing the inlet temperature would cause a change in the boiling length as calculated from a heat balance; (c) the EG/W mixture of the higher ethylene glycol volume concentration generally boils at a higher wall superheat for the same heat flux, or at a lower heat flux for the same wall superheat; and (d) to reach the same wall superheat, the heat fluxes for vertical upward flow

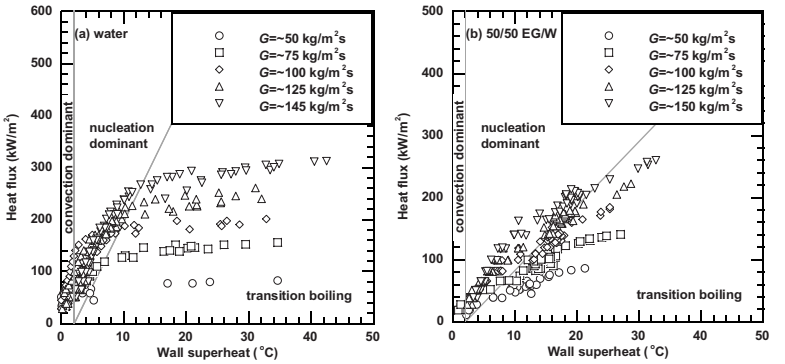

FIG. 5—*Three regions in small-channel boiling.*

boiling are higher than those for horizontal flow boiling, which is attributed to the vapor distribution for vertical upward flow boiling being more uniform than that for horizontal flow boiling due to the influence of gravity in horizontal flow boiling.

Boiling Heat Transfer Coefficient Comparison

Many equations for heat transfer coefficients of internal forced convective boiling with pure component fluids and mixtures have been developed such as those documented in review papers [27–32]. These equations usually pertain to a range of working fluids, flow channel geometries, heat fluxes, mass fluxes, and system pressures and can generally be divided into three types. The first type is the enhancement model that treats two-phase phenomena as a kind of perturbation to single-phase heat transfer, and such equations utilize a form of single-phase convective heat transfer equations, modified to include boiling impact [33–37]. The second type is the superposition model or the asymptotic model that uses the superposition or the power-type superposition of convective heat transfer and nucleation-boiling heat transfer to account for two-phase heat transfer [18,38–44]. The third type is the nucleation-domination model that contains only a nucleation term or exhibits a heat flux but no mass flux dependence [22,24,25,45–47].

Four equations from the engineering literature were chosen as most appropriate to analyze the experimental heat transfer coefficients of water and EG/W mixture flow boiling of this study [22,36,38,41]. In Figs. 6 and 7, the experimental heat transfer coefficients of water and EG/W mixture flow boiling of this study are compared to the predictions from these equations. It can be seen from Figs. 6 and 7 that (a) all equations correctly predict the trend of the experimental heat transfer coefficients of water flow boiling of this study, which is expected because the heat transfer coefficient databases for water flow boiling were used in developing these equations; (b) generally, the predictions for vertical upward water flow boiling are better than those for horizontal water flow boiling, which may be explained by the fact that vertical upward flow boiling is more stable than horizontal flow boiling due to the symmetrical boiling condition without gravitational effects; (c) for vertical upward water flow boiling, almost all equations predict the experimental heat transfer coefficients reasonably well, while for horizontal water flow boiling, the Gungor–Winterton equation [41] gives the best prediction for the experimental heat transfer coefficients of this study; (d) the predictions for the experimental heat transfer coefficients of EG/W mixture flow boiling of this study generally are not satisfactory which may be due to the fact that the boiling complications of two- or multi-component fluids such as EG/W mixtures were not taken into account in developing most of these equations; and (e) the best predictions for the experimental heat transfer coefficients of EG/W mixture flow boiling of this study are given by the equation developed based on the horizontal water and 50/50 EG/W mixture flow boiling data of Yu et al. [22], but the discrepancies between the experimental data and the predicted values are still rather large. (Note that the data of Fig. 7 include all three concentrations of EG/W mixtures.) Comparisons between the experimental data and the predicted values from other equations [33,34,40,43,46,47] were also made and similar results to the above comparisons were observed. Therefore, further data analyses and correlation development were necessary.

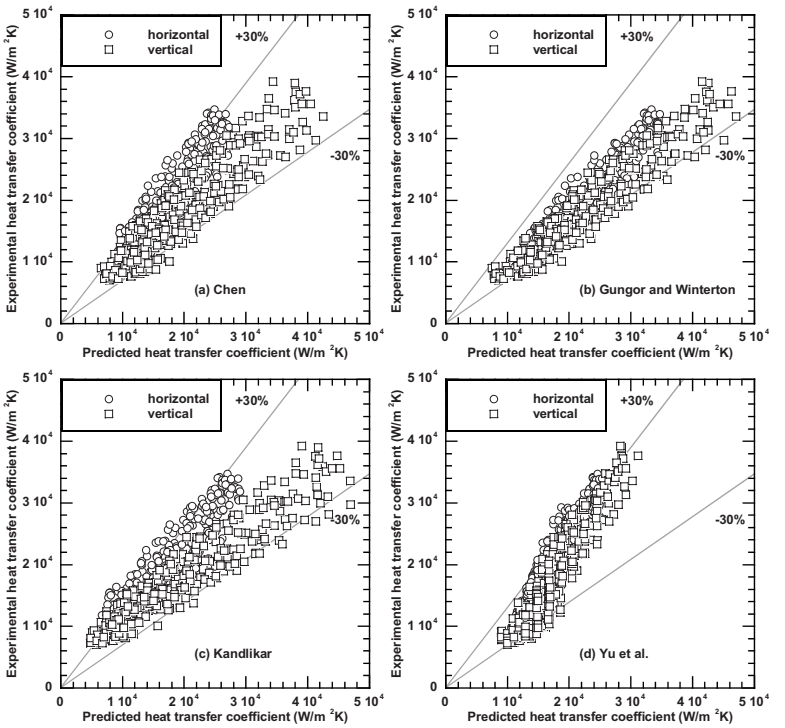

FIG. 6—*Heat transfer coefficient comparison of water boiling.*

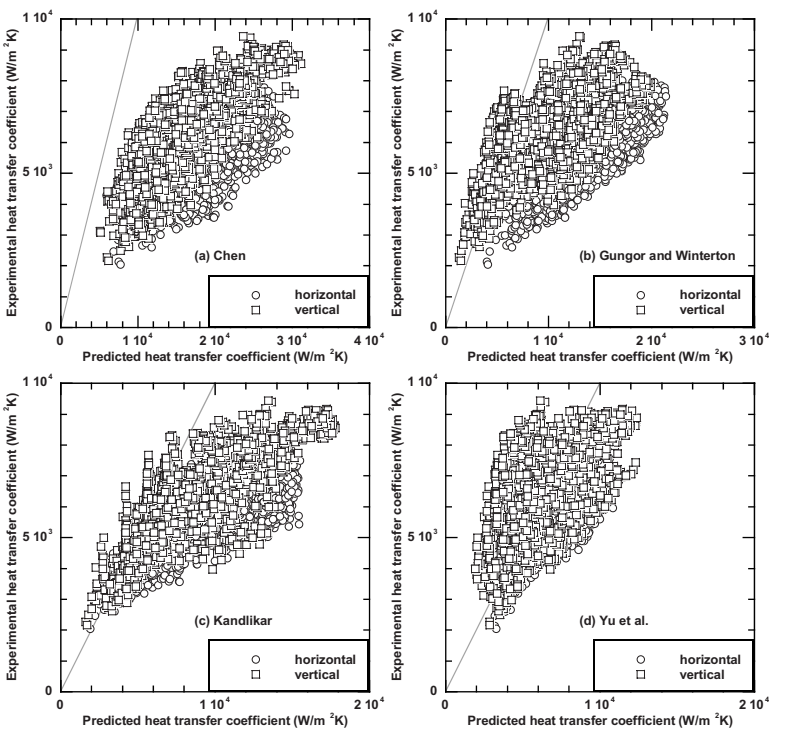

FIG. 7—*Heat transfer coefficient comparison of EG/W mixture boiling.*

Correlation of Experimental Boiling Heat Transfer Coefficient

In correlating the experimental boiling heat transfer coefficients of this study, the following facts are taken into account: (a) The goal is to develop simple and practically useful equations for water and EG/W mixture flow boiling of this study; (b) while both convective and nucleate-boiling heat transfer exist, the dominant heat transfer mechanism for the experimental data of this study is nucleate boiling; (c) as shown previously, the boiling heat transfer is dependent on the heat flux but almost independent of the mass flux;

and (d) the heat transfer coefficients have different dependences on heat flux for different fluids, and therefore it is necessary to include the effects of fluid thermal properties or the ethylene glycol volume concentration or both to get a general equation for predicting all boiling heat transfer coefficients of this study.

A prediction equation for the boiling heat transfer coefficient was developed based on the experimental heat transfer coefficients of water and EG/W mixture flow boiling of this study through the following steps. (a) Based on the characteristics of the experimental boiling heat transfer coefficients of this study, a dimensionless combination form $\mathrm{BoWe}_l^{0.5} = \dot{q}'' d_i^{0.5} / (\rho_l^{0.5} i_{fg} \sigma^{0.5})$ of Boiling number $\mathrm{Bo} = \dot{q}'' / (G i_{fg})$ and liquid Weber number $We_l = G^2 d_i / (\rho_l \sigma)$ was chosen to be the primary correlating parameter [22,24,25]. It was found that the heat transfer coefficients of water and EG/W flow boiling of this study follow different trends from each other. (b) The experimental boiling heat transfer coefficients were nondimensionalized by dividing them by (k_l / d_i) where k_l is the liquid thermal conductivity and d_i is the inside test section diameter. This process not only narrowed the distribution range of the experimental boiling heat transfer coefficients but also reduced the experimental boiling heat transfer coefficient gap between water flow boiling and EG/W mixture flow boiling. (c) Various combinations of the thermal properties and the ethylene glycol volume concentration of the experimental fluids were tested in an attempt to merge the experimental heat transfer coefficients of water flow boiling and EG/W mixture flow boiling of this study, and it was found that a simple exponential factor $(e^{1.25 V_{\mathrm{EG}}})$ of the ethylene glycol volume concentration V_{EG} works quite well. This exponential factor reduces to unity for pure water with the ethylene glycol volume concentration of zero. (d) The final equation developed based on the experimental heat transfer coefficients of water and EG/W mixture boiling in both horizontal and vertical upward flows of this study is

$$h = 3200 e^{-1.25 V_{\mathrm{EG}}} (\mathrm{BoWe}_l^{0.5})^{0.45} (k_l / d_i) \tag{13}$$

As seen from Fig. 8(*a*), where the experimental boiling heat transfer coefficients are compared with the predictions of the above equation, Eq 13 predicts the experimental boiling heat transfer coefficients of this study reasonably well with mean deviations of 22 % for water flow boiling, 25 % for EG/W mixture flow boiling, and 25 % for overall water and EG/W mixture flow boiling. The majority of the experimental boiling heat transfer coefficients are within ±30 % of the predictions.

The prediction accuracy can be improved if the experimental heat transfer coefficients of water flow boiling and EG/W mixture flow boiling of this study are separately correlated. The final equation developed based on the experimental heat transfer coefficients of water boiling in both horizontal and vertical upward flows of this study is

$$h = 25\,770 (\mathrm{BoWe}_l^{0.5})^{0.7} (k_l / d_i) \tag{14}$$

As seen from Fig. 8(*b*), where the experimental boiling heat transfer coefficients are compared with the predictions of the above equation, Eq 14 predicts the experimental water boiling heat transfer coefficients of this study reasonably well with a mean deviation of 16 %, and most of the experimental boiling heat transfer coefficients are within ±30 % of the predictions.

The final equation developed, based on the experimental heat transfer coefficients of EG/W mixture flow boiling in both horizontal and vertical upward flows of this study, is

$$h = 1650 (\mathrm{BoWe}_l^{0.5})^{0.45} (k_l / d_i) \tag{15}$$

As seen from Fig. 8(*c*), where the experimental boiling heat transfer coefficients are compared with the predictions of the above equation, Eq 15 predicts the experimental EG/W boiling heat transfer coefficients of this study reasonably well with mean deviations of 16 % for horizontal flow, 13 % for vertical upward flow, and 14 % for overall EG/W mixture flow boiling. The majority of the experimental boiling heat transfer coefficients are within ±30 % of the predictions for all three concentrations tested.

The prediction accuracy can be further improved if the experimental heat transfer coefficients of EG/W mixture boiling in horizontal flow and vertical upward flow of this study are separately correlated. The final equation developed, based on the experimental heat transfer coefficients of EG/W mixture boiling in horizontal flow of this study, is

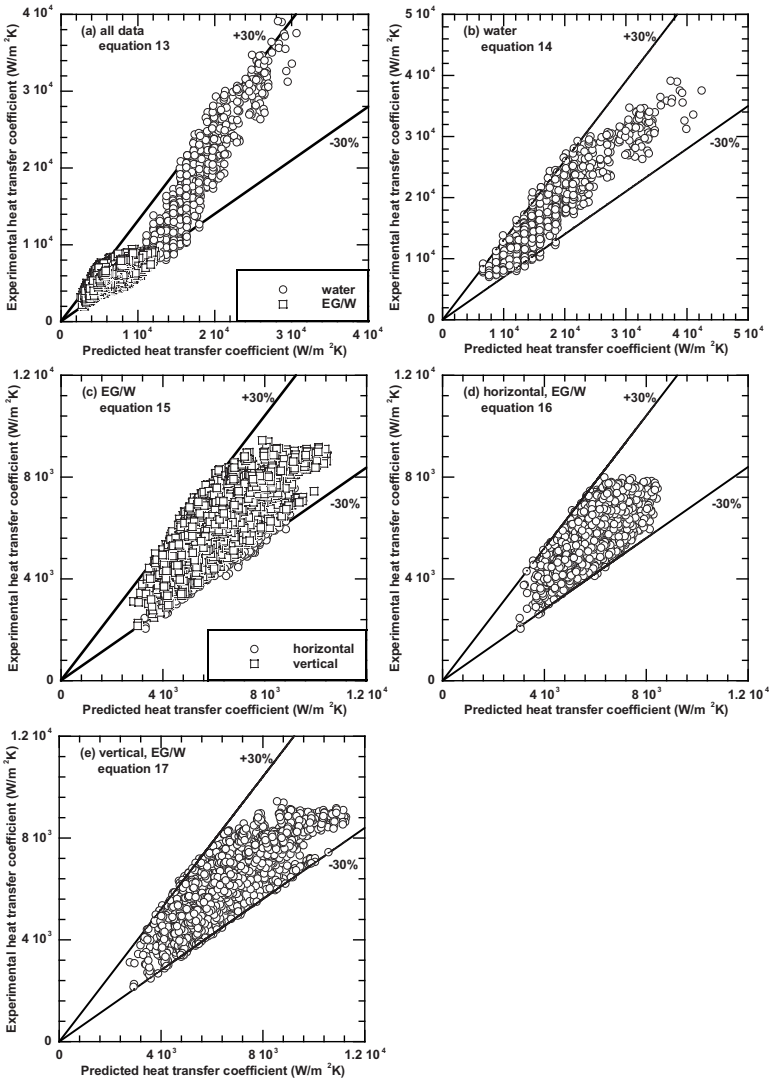

FIG. 8—*New heat transfer coefficient comparisons.*

$$h = 1520(\mathrm{BoWe}_l^{0.5})^{0.45}(k_l/d_i) \tag{16}$$

As seen from Fig. 8(*d*), where the experimental boiling heat transfer coefficients are compared with the predictions of the above equation, Eq 16 predicts the experimental EG/W horizontal boiling heat transfer coefficients of this study reasonably well with a mean deviation of 11 %, and most of the experimental boiling heat transfer coefficients are within ±30 % of the predictions. The final equation developed, based on the experimental heat transfer coefficients of EG/W mixture boiling in the vertical upward flow of this study, is

$$h = 2350(\mathrm{BoWe}_l^{0.5})^{0.49}(k_l/d_i) \tag{17}$$

As seen from Fig. 8(*e*), where the experimental boiling heat transfer coefficients are compared with the predictions of the above equation, Eq 17 predicts the experimental EG/W vertical upward flow boiling heat transfer coefficients of this study reasonably well with a mean deviation of 12 %, and most of the experimental boiling heat transfer coefficients are within ±30 % of the predictions.

It should be noted that Eqs 13–17 were correlated based on the experimental data of this study for the test section diameter of 2.98 mm. It is expected that these equations will be valid for flow systems with a similar diameter. However, precaution should be taken when they are applied for flow systems with a much different diameter.

Conclusions

A series of experiments was carried out to investigate forced convective boiling heat transfer characteristics under conditions of small channels and low mass fluxes for distilled water and EG/W mixtures with volume concentration ratios of 40/60, 50/50, and 60/40 in both horizontal and vertical upward flows. The following conclusions can be drawn from the experimental data and analyses.

(i) A boiling data reduction procedure has been developed that allows the accurate calculation of the fluid boiling temperatures along the experimental test section and subsequently the local boiling heat transfer coefficients by applying ideal mixture and equilibrium assumptions along with Raoult's law. Due to its analytical nature, this procedure can easily be adapted for designing practical cooling systems with flow boiling.

(ii) The experimental data show that (a) the system pressure has a very slight effect on the exit boiling curves for the two test section outlet pressure of 150 and 200 kPa; (b) under the current test conditions, the exit boiling curves are insensitive to the test section inlet temperature although changing the inlet temperature would cause a change in the boiling length as calculated from a heat balance; (c) the EG/W mixture of the higher ethylene glycol volume concentration generally boils at a higher wall superheat for the same heat flux, or at a lower heat flux for the same wall superheat; and (d) to reach the same wall superheat, the heat fluxes for vertical upward flow boiling are higher than those for horizontal flow boiling, which is attributed to the vapor distribution for vertical upward flow boiling being more uniform than that for horizontal flow boiling due to the influence of gravity in horizontal flow boiling.

(iii) Flow boiling in small channels can be characterized according to three boiling regions. In the convection-dominant-boiling region where the wall superheat is less than 2°C, the heat fluxes are relatively independent of the wall superheat, and the flow acts more like single-phase rather than two-phase. In the nucleation-dominant-boiling region, the heat flux is dependent on the wall superheat but almost independent of the mass flux. In the transition-boiling region where the wall superheat is highest, the wall temperatures show oscillations, the heat fluxes separate as a function of the mass flux, and the flow boiling is susceptible to flow instabilities. At high enough wall superheats, the critical heat flux condition will be reached.

(iv) The large nucleation-dominant-boiling region, which is the focus of this study, is the generally desired operating region for flow boiling in small channels. This situation is due to the relatively high heat transfer rates and flow stability. In the nucleation-dominant-boiling region, the heat fluxes follow a strong power-law trend of the wall superheat nearly independent of the mass flux, which, coupled with the negligible inlet temperature effect, implies that the nucleate-boiling heat transfer coefficients up to the transition-boiling region are a function of the heat flux only but not a function of the mass flux or the inlet subcooling. These phenomena indicate the domination of the nucleation heat transfer mechanism and the minimization of the convective heat transfer mechanism over a large mass flux range and a large inlet-subcooling range.

(v) For vertical upward flow, most equations from the literature predict the experimental heat transfer coefficients of water boiling of this study reasonably well, while for horizontal flow, the Gungor-Winterton equation gives the best prediction. Generally, the predictions for vertical upward flow boiling of water are better than those for horizontal flow boiling, which may be explained by the fact that vertical upward flow boiling is more stable than horizontal flow boiling due to the symmetrical boiling condition without gravitational effects.

(vi) No equations from the literature predicted the experimental heat transfer coefficients well for the EG/W mixture flow boiling of this study, which may be due to the fact that the complex boiling conditions of two- or multi-component fluids such as EG/W mixtures were not taken into account in developing those equations.

(vii) Five prediction equations for boiling heat transfer coefficients have been developed based on the experimental water and EG/W mixture flow boiling data of this study including (a) a general equation for both water and EG/W mixture boiling in horizontal and vertical upward flows with a mean deviation of 25 %, (b) an equation for water boiling in horizontal and vertical upward flows with a mean deviation of 16 %, (c) an equation for EG/W mixture boiling in horizontal and vertical upward flows with a mean deviation of 14 %, (d) an equation for EG/W mixture

boiling in horizontal flow with a mean deviation of 11 %, and (e) an equation for EG/W mixture boiling in vertical upward flow with a mean deviation of 12 %.

References

[1] Finlay, I. C., Boyle, R. J., Pirault, J. P., and Biddulph, T., 1987, "Nucleate and Film Boiling of Engine Coolants Flowing in a Uniformly Heated Duct of Small Cross Section," *SAE Technical Paper 870032*, Washington D.C.

[2] Finlay, I. C., Gallacher, G. R., Biddulph, T. W., and Marshall, R. A., 1988, "The Application of Precision Cooling to the Cylinder Head of a Small Automotive Petrol Engine," *SAE Technical Paper 880263*, Washington D.C.

[3] Clough, M. J., 1993, "Precision Cooling of a Four Valve per Cylinder Engine," *SAE Technical Paper 931123*, Washington D.C.

[4] Pretscher, M. and Ap, N. S., 1993, "Nucleate Boiling Engine Cooling System—Vehicle Study," *SAE Technical Paper 931132*, Washington D.C.

[5] Gentile, D. and Zidat, S., "Influential Parameters in a Boiling Cooling System," *Heat Technol.*, Vol. 11, 1993, pp. 28–51.

[6] McAssey, E. V., Stinson, C., and Gollin, M., "Evaluation of Engine Coolants Under Flow Boiling Conditions," *Proceedings of the ASME Heat Transfer Division*, Vol. 317-1, San Francisco, CA, November 12–17, ASME, New York, 1995, pp. 193–200.

[7] Campbell, N. A. F., Charlton, S. J., and Wong, L., 1995, "Designing Towards Nucleate Boiling in Combustion Engines," *IMechE Paper C496/092/95*, London.

[8] Campbell, N. A. F., Tilley, D. G., MacGregor, S. A., and Wong, L., 1997, "Incorporating Nucleate Boiling in a Precision Cooling Strategy for Combustion Engines," *SAE Technical Paper 971791*, Washington D.C.

[9] Ambrogi, G., McAssey, E. V., Cozzone, G., and Hoover, C., 1997, "The Effect of Off-Design Operation on the Thermal Performance of Propylene-Glycol and Ethylene-Glycol Engine Coolants," *SAE Technical Paper 971827*, Washington D.C.

[10] Campbell, N. A. F., Hawley, J. G., Tilley, D. G., Wong, L., and Horrocks, R. W., 1999, "Nucleate Boiling Investigations Using Simulated Engine Cooling Passages," *IMechE Paper C543/002/99*, London.

[11] Ap, N. S., Maire, A., Porot, P., Menegazzi, P., Souidi, F., Devehat, C. L., Godeau, D., Olivier, P., Vinot, J. B., and Vincens, G., 1999, "New Components Development for New Engine Cooling System," *IMechE Paper C543/047/99*, London.

[12] Wambsganss, M. W., 1999, "Thermal Management in Heavy Vehicles: A Review Identifying Issues and Research Requirements," *IMechE Paper C543/086/99*, London.

[13] Campbell, N. A. F., Hawley, J. G., Leathard, M. J., Horrocks, R. W., and Wong, L., 1999, "Nucleate Boiling Investigations and the Effects of Surface Roughness," *SAE Technical Paper 1999-01-0577*, Washington D.C.

[14] Robinson, K., Campbell, N. A. F., Hawley, J. G., and Tilley, D. G., 1999, "A Review of Precision Engine Cooling," *SAE Technical Paper 1999-01-0578*, Washington, D.C.

[15] Wambsganss, M. W., 1999, "Thermal Management Concepts for Higher-Efficiency Heavy Vehicles," *SAE Technical Paper 1999-01-2240*, Washington D.C.

[16] Gnielinski, V. V., "Neue Gleichungen für den Wärme-und den Stoffübergang in turbulent durchströmten Rohren und Kanälen [New Equations for Heat and Mass Transfer in Turbulent Flow through Pipes and Ducts]," *Forschung im Ingenieurwesen*, Vol. 41, 1975, pp. 8–16.

[17] Chu, J. C., Wang, S. L., Levy, S. L., and Paul, R., *Vapor-Liquid Equilibrium Data*, J.W. Edwards Publisher, Inc., Ann Arbor, MI, 1956.

[18] Murata, K. and Hashizume, K., "An Investigation on Forced Convection Boiling of Nonazeotropic Refrigerant Mixtures," *Heat Transfer-Jpn. Res.*, Vol. 19, 1990, pp. 95–109.

[19] Wenzel, U., Hartmuth, B., and Muller-Steinhagen, H., "Heat Transfer to Mixtures of Acetone, Isopropanol and Water Under Subcooled Flow Boiling Conditions—I. Experimental Results," *Int. J. Heat Mass Transfer*, Vol. 37, 1994, pp. 175–183.

[20] Morrison, G. and McLinden, M. O., 1986, "Application of a Hard Sphere Equation of State to

Refrigerants and Refrigerant Mixtures," *National Bureau of Standards Technical Note 1226*, Gaithersburg, MD.

[21] Ross, H., Radermacher, R., di Marzo, M., and Didion, D., "Horizontal Flow Boiling of Pure and Mixed Refrigerants," *Int. J. Heat Mass Transfer*, Vol. 30, 1987, pp. 979–992.

[22] Yu, W., France, D. M., Ramamoorthy, V.-K. V., and Hull, J. H., "Small-Channel Flow Boiling of One-Component Fluids and an Ethylene Glycol/Water Mixture," *Exp. Heat Transfer*, Vol. 18, 2005, pp. 243–257.

[23] Moffat, R. J., "Describing the Uncertainties in Experimental Results," *Exp. Therm. Fluid Sci.*, Vol. 1, 1988, pp. 3–17.

[24] Yu, W., France, D. M., Wambsganss, M. W., and Hull, J. R., "Two-Phase Pressure Drop, Boiling Heat Transfer, and Critical Heat Flux to Water in a Small-Diameter Horizontal Tube," *Int. J. Multiphase Flow*, Vol. 28, 2002, pp. 927–941.

[25] Tran, T. N., Wambsganss, M. W., and France, D. M., "Small Circular- and Rectangular-Channel Boiling with Two Refrigerants," *Int. J. Multiphase Flow*, Vol. 22, 1996, pp. 485–498.

[26] Wambsganss, M. W., Jendrzejczyk, J. A., and France, D. A., 1992, "Two-Phase Flow and Pressure Drop in Flow Passages of Compact Heat Exchangers," *SAE Technical Paper 920550*, Washington D.C.

[27] Thome, J. R. and Shock, R. A. W., "Boiling of Multicomponent Liquid Mixtures," *Advances in Heat Transfer*, J. P. Hartnett and T. F. Irvine Jr., Eds., Academic Press, New York, Vol. 16, 1984, pp. 59–156.

[28] Webb, R. L. and Gupte, N. S., "A Critical Review of Correlations for Convective Vaporization in Tubes and Tube Banks," *Heat Transfer Eng.*, Vol. 13, 1992, pp. 58–81.

[29] Celata, G. P., Cumo, M., and Setaro, T., "A Review of Pool and Forced Convective Boiling of Binary Mixtures," *Exp. Therm. Fluid Sci.*, Vol. 9, 1994, pp. 367–381.

[30] Darabi, J., Salehi, M., Saeedi, M. H. and Ohadi, M. M., "Review of Available Correlations for Prediction of Flow Boiling Heat Transfer in Smooth and Augmented Tubes," *ASHRAE Transactions*, Vol. 101, Part 1, Paper No. CH-95-12-2, ASHRAE, Atlanta, GA, 1995, pp. 225–235.

[31] Wang, S. P. and Chato, J. C., "Review of Recent Research on Heat Transfer with Mixtures—Part 2: Boiling and Evaporation," *ASHRAE Transactions*, Vol. 101, Part 1, Paper No. CH-95-23-3, ASHRAE, Atlanta, GA, 1995, pp. 1387–1401.

[32] Bertsch, S. S., Groll, E. A., and Garimella, S. V., "Review and Comparative Analysis of Studies on Saturated Flow Boiling in Small Channels," *Nanoscale Microscale Thermophys. Eng.*, Vol. 12, 2008, pp. 187–227.

[33] Shah, M. M., "A New Correlation for Heat Transfer During Boiling Flow Through Pipes," *ASHRAE Trans.*, Vol. 82, 1976, pp. 66–86.

[34] Shah, M. M., "Chart Correlation for Saturated Boiling Heat Transfer: Equations and Further Study," *ASHRAE Trans.*, Vol. 88, 1982, pp. 185–196.

[35] Mishra, M. P., Varma, H. K., and Sharma, C. P., "Heat Transfer Coefficients in Forced Convection Evaporation of Refrigerants Mixtures," *Lett. Heat Mass Transfer*, Vol. 8, 1981, pp. 127–136.

[36] Kandlikar, S. G., "A General Correlation for Saturated Two-Phase Flow Boiling Heat Transfer Inside Horizontal and Vertical Tubes," *ASME Trans. J. Heat Transfer*, Vol. 112, 1990, pp. 219–228.

[37] Takamatsu, H., Miyara, A., Koyama, S., Fujii, T., and Yonemoto, K., "Forced Convective Boiling of Nonazeotropic Refrigerant Mixtures of R22 and R114 Inside a Horizontal Tube," *Heat Transfer-Jpn. Res.*, Vol. 19, 1990, pp. 68–82.

[38] Chen, J. C., "Correlation for Boiling Heat Transfer to Saturated Fluids in Convective Flow," *Ind. Eng. Chem. Process Des. Dev.*, Vol. 5, 1966, pp. 322–329.

[39] Bennett, D. L. and Chen, J. C., "Forced Convective Boiling in Vertical Tubes for Saturated Pure Components and Binary Mixtures," *AIChE J.*, Vol. 26, 1980, pp. 454–461.

[40] Bjorge, R. W., Hall, G. R., and Rohsenow, W. M., "Correlation of Forced Convection Boiling Heat Transfer Data," *Int. J. Heat Mass Transfer*, Vol. 25, 1982, pp. 753–757.

[41] Gungor, K. E. and Winterton, R. H. S., "A General Correlation for Flow Boiling in Tubes and Annuli," *Int. J. Heat Mass Transfer*, Vol. 29, 1986, pp. 351–358.

[42] Jung, D. S., McLinden, M., Radermacher, R., and Didion, D., "A Study of Flow Boiling Heat Transfer with Refrigerant Mixtures," *Int. J. Heat Mass Transfer*, Vol. 32, 1989, pp. 1751–1764.

[43] Liu, Z. and Winterton, R. H. S., "A General Correlation for Saturated and Subcooled Flow Boiling in Tubes and Annuli, Based on a Nucleate Pooling Boiling Equation," *Int. J. Heat Mass Transfer*, Vol. 34, 1991, pp. 2759–2766.

[44] Steiner, D. and Taborek, J., "Flow Boiling Heat Transfer in Vertical Tubes Correlated by a Asymptotic Model," *Heat Transfer Eng.*, Vol. 13, 1992, pp. 43–69.

[45] Lazarek, G. M. and Black, S. H., "Evaporative Heat Transfer, Pressure Drop and Critical Heat Flux in a Small Vertical Tube with R-113," *Int. J. Heat Mass Transfer*, Vol. 25, 1982, pp. 945–960.

[46] Klimenko, V. V., "A Generalized Correlation for Two-Phase Forced Flow Heat Transfer," *Int. J. Heat Mass Transfer*, Vol. 31, 1988, pp. 541–552.

[47] Klimenko, V. V., "A Generalized Correlation for Two-Phase Forced Flow Heat Transfer-Second Assessment," *Int. J. Heat Mass Transfer*, Vol. 33, 1990, pp. 2073–2088.